

# *In situ* measurements of atmospheric NO<sub>2</sub> using incoherent broadband cavity-enhanced absorption spectroscopy with a blue light-emitting diode

Liuyi Ling (凌六一)<sup>1,2</sup>, Pinhua Xie (谢品华)<sup>1\*</sup>, Min Qin (秦敏)<sup>1</sup>, Wu Fang (方武)<sup>1</sup>, Yu Jiang (江宇)<sup>1</sup>, Renzhi Hu (胡仁志)<sup>1</sup>, and Nina Zheng (郑尼娜)<sup>1</sup>

<sup>1</sup>Anhui Institute of Optics and Fine Mechanics, Key Laboratory of Environmental Optics and Technology, Chinese Academy of Science, Hefei 230031, China

<sup>2</sup>Institute of Electric and Information Technology, Anhui University of Science and Technology, Huainan 232001, China

\*Corresponding author: phxie@aiofm.ac.cn

Received November 29, 2012; accepted February 25, 2012; posted online May 30, 2013

We describe the application of incoherent broadband cavity-enhanced absorption spectroscopy (IBBCEAS) for *in situ* measurements of atmospheric NO<sub>2</sub> using a blue light-emitting diode. The mirror reflectivity is determined by the transmitted intensity variation through the cavity caused by Rayleigh scattering. Concentrations of atmospheric NO<sub>2</sub> (1 to 35 ppbv) during the seven-day period are retrieved from the absorption spectra. The IBBCEAS measurement data are compared with those of a commercial long path differential optical absorption spectroscopy. The linear regression has a correlation coefficient and a slope of 0.983 and 0.975, respectively.

OCIS codes: 300.1030, 300.6470, 120.4640.

doi: 10.3788/COL201311.063001.

NO<sub>2</sub>, one of the trace gases in the atmosphere, plays an important role in atmospheric chemistry. This gas is also an atmospheric pollutant that can cause acid rain and photochemical smog, impairing human health. Thus, measuring atmospheric NO<sub>2</sub> concentration is essential for both atmospheric chemistry research and air quality management and control.

Differential optical absorption spectroscopy (DOAS) is a common spectroscopic technology for measuring NO<sub>2</sub><sup>[1]</sup> that has been successfully applied in trace gas measurements for several decades. A direct approach to improve detection sensitivity in DOAS is to enhance the optical absorption length. For example, active long path DOAS (LP-DOAS)<sup>[2]</sup> instruments are used to realize long optical paths in the atmosphere from several hundred meters to more than 20 km. These long paths are necessary to detect gases with mixing ratios in the pptv to ppbv range by DOAS in the UV-visible spectral range.

Incoherent broadband cavity-enhanced absorption spectroscopy (IBBCEAS)<sup>[3]</sup> based on cavity-ring down spectroscopy (CRDS)<sup>[4]</sup> has been rapidly developed in recent years. Although the IBBCEAS instrumental setup is much more compact than LP-DOAS, its detection sensitivity can be as high as that of LP-DOAS. Light-emitting diodes (LEDs) are often used as optical sources of IBBCEAS because their emission spectra can be matched to the expected reflectivity of mirrors in the IBBCEAS setup. Ball *et al.*<sup>[5]</sup> measured NO<sub>2</sub> and NO<sub>3</sub> samples using IBBCEAS with a red LED. Langridge *et al.*<sup>[6]</sup> measured NO<sub>2</sub> in the laboratory air for 38 h using IBBCEAS with a blue LED. Wu *et al.*<sup>[7]</sup> measured HONO and NO<sub>2</sub> in ambient air in an urban environment at modest aerosol levels using open-path IBBCEAS with a near-UV LED. Our group has developed a custom-made IBBCEAS system based on LEDs to successfully detect several samples

in the laboratory<sup>[8,9]</sup>.

IBBCEAS has been used to measure various trace gases such as NO<sub>2</sub><sup>[5–8,10–12]</sup>, NO<sub>3</sub><sup>[5,11–15]</sup>, N<sub>2</sub>O<sub>5</sub><sup>[15]</sup>, HONO<sup>[7,9,10]</sup>, O<sub>3</sub><sup>[11]</sup>, I<sub>2</sub><sup>[5]</sup>, IO<sup>[14]</sup>, and CHOCHO<sup>[14]</sup>. However, this technique is not frequently applied for long-term measurements. This letter reports on a seven-day continuous measurement of atmospheric NO<sub>2</sub> using IBBCEAS with a blue LED. Based on the fitting residuals, the average detection limit of NO<sub>2</sub> is 1.8 ppbv for an acquisition time of 90 s.

Fiedler *et al.*<sup>[3]</sup> described the principle of quantifying trace gas concentrations with IBBCEAS. The absorption coefficient of the measured gases,  $\alpha_{\text{abs}}(\lambda)$ , is related to the light intensity transmitted through the cavity, i.e.,

$$\alpha_{\text{abs}}(\lambda) = \sum_i \sigma_i(\lambda) \cdot N_i = \left[ \frac{1 - R(\lambda)}{d} + \alpha_{\text{Ray}}(\lambda) \right] \left[ \frac{I_0(\lambda) - I(\lambda)}{I(\lambda)} \right]. \quad (1)$$

The extinction caused by aerosols is not considered.  $R(\lambda)$  is the wavelength resolved mirror reflectivity, and  $d$  is the length of the cavity.  $\alpha_{\text{Ray}}(\lambda)$  is the total Rayleigh scattering for the mixture.  $I(\lambda)$  and  $I_0(\lambda)$  are the measured spectra with and without absorbing species in the cavity, respectively.  $\sigma_i(\lambda)$  is the absorption cross-section, and  $N_i$  is the number density for species  $i$ . The concentrations of the measured gases can be retrieved by fitting the absorption cross-sections to the absorption coefficient.

Figure 1 shows the schematic of the IBBCEAS instrumental setup. A blue LED (XRE-7090, CREE, USA) with a peak wavelength of approximately 462 nm and a full-width at half-maximum (FWHM) of 26 nm was used as the light source. The LED working current was 700

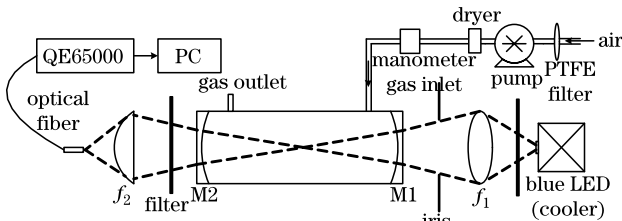


Fig. 1. Schematic of the IBBCEAS instrumental setup.

$\pm 1$  mA, which provided an optical power of  $\sim 600$  mW. The LED was mounted on a temperature-controlled cooling stage to stabilize its emission spectrum. Through the lens  $f_1$  ( $f = 352$  mm), the light emitted from the LED was focused into a 70-cm-long high-finesse cavity. This cavity consisted of two high-reflectivity dielectric mirrors (Layertec GmbH) with a high reflectivity of over 0.999 from 440 to 480 nm, 25-mm diameter, and 1.5-m radius of curvature. An iris was used to reduce the stray light and confine the diameter of the light spot on the first mirror (M1). Out-of-band light was removed by a colored glass filter (GG420, Schott, Germany) behind the LED and a band-pass filter (BQ29, Yinxing Optics, China) behind the second mirror (M2). Light transmitted through M2 was focused into an optical fiber (400  $\mu\text{m}$  in diameter and  $\text{NA} = 0.22$ ) connected to a 0.3-nm resolution spectrometer (QE65000, Ocean Optics, USA) by an aspheric lens  $f_2$  ( $f = 32$  mm). The sampled air was filtered by a PTFE filter (pore size 0.22  $\mu\text{m}$ ) to remove aerosols and pumped at a flow rate of 3 slm through a 21-mm internal diameter Teflon-coated tube into the cavity. Atmospheric absorption spectra were recorded and analyzed by a PC. Although the pump (NMP850, KNF, Germany) is generally placed on the outlet side, the pump in the present system was placed on the inlet side to maintain a positive pressure and reduce sampling artefacts from ingress of laboratory aerosols into the optical cavity.

Mirror reflectivity should be determined to quantify gas concentrations based on Eq. (1). Langridge *et al.*<sup>[16]</sup> determined the mirror reflectivity by measuring the ring-down time of CRDS. Gherman *et al.*<sup>[10,17]</sup> acquired the reflectivity using the absorption spectrum of a known concentration gas in the region of interest. In addition, mirror reflectivity can be determined from the light intensity changes caused by the addition of  $\text{N}_2$  and He, as described by Washenfelder *et al.*<sup>[18]</sup>

$$R(\lambda) = 1 - d \frac{\left[ \frac{I_{\text{N}_2}(\lambda)}{I_{\text{He}}(\lambda)} \alpha_{\text{Ray}}^{\text{N}_2}(\lambda) \right] - [\alpha_{\text{Ray}}^{\text{He}}(\lambda)]}{1 - \left[ \frac{I_{\text{N}_2}(\lambda)}{I_{\text{He}}(\lambda)} \right]}, \quad (2)$$

where  $I_{\text{N}_2}(\lambda)$  and  $I_{\text{He}}(\lambda)$  are the  $\text{N}_2$  and He spectral intensities, respectively;  $\alpha_{\text{Ray}}^{\text{He}}(\lambda)$  and  $\alpha_{\text{Ray}}^{\text{N}_2}(\lambda)$  are the extinction coefficients caused by Rayleigh scattering of He and  $\text{N}_2$ , respectively.

This letter determined the mirror reflectivity using the last method.  $I_{\text{N}_2}(\lambda)$  and  $I_{\text{He}}(\lambda)$  were recorded by QE65000 at ambient temperature (297 K) and pressure (1013 mbar) after the cavity was flushed with pure  $\text{N}_2$  (99.999% purity) and pure He (99.999% purity), respectively.  $\alpha_{\text{Ray}}^{\text{He}}(\lambda)$  and  $\alpha_{\text{Ray}}^{\text{N}_2}(\lambda)$  were acquired by calculation. Thus,  $\alpha_{\text{Ray}}(\lambda) = \sigma_{\text{Ray}}(\lambda) \cdot N$ , where  $N$  is the number density and related to purity of He or  $\text{N}_2$ .  $\sigma_{\text{Ray}}(\lambda)$  is

the Rayleigh scattering cross-sections of He or  $\text{N}_2$ . According to Shardanand *et al.*<sup>[19]</sup> who measured  $\sigma_{\text{Ray}}^{\text{He}}$  at 457.9 nm, and Sneep *et al.*<sup>[20]</sup> who measured  $\sigma_{\text{Ray}}^{\text{N}_2}$  at 532 nm, and based on wavelength dependence to an expression ( $\sigma_{\text{Ray}}(\lambda) \sim \lambda^{-4.082}$ ),  $\sigma_{\text{Ray}}(\lambda)$  is interpolated to obtain cross-section values over the region of interest. Figure 2(b) shows the extinction caused by Rayleigh scattering of pure He and  $\text{N}_2$  in our experiments. The calibrated mirror reflectivity in the region from 443 to 470 nm is shown in Fig. 2(a). The maximum mirror reflectivity of 0.9987 is found at 458 nm, which corresponds to an effective path length of  $\sim 538$  m. Although the difference in the  $\text{N}_2$  and He spectral intensities in Fig. 2(a) is small ( $\sim 2\%$ ), it is far more than 0.1% of the average change in the intensities of the consecutive  $\text{N}_2$  spectra acquired by the spectrometer. Thus, this intensity difference is reliable in determining mirror reflectivity.

Atmospheric  $\text{NO}_2$  samples obtained outside our laboratory were measured continuously for seven days using the IBBCEAS instrument and a commercial LP-DOAS system. Other absorptions such as ozone, water vapor, and  $\text{O}_2\text{-O}_2$  collisional pair also exist in the spectral range (443–470 nm) used for  $\text{NO}_2$  concentration retrieval

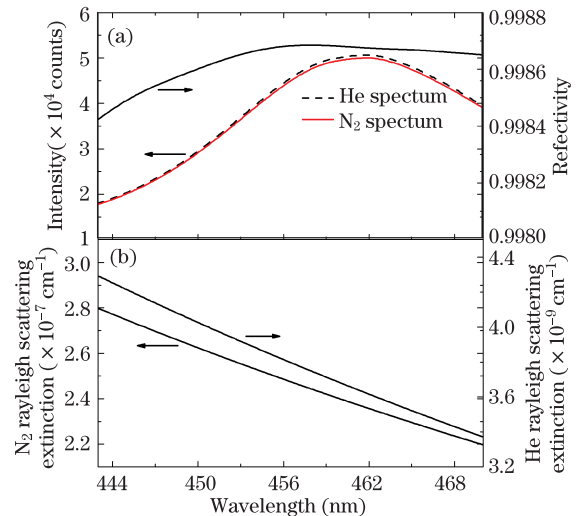


Fig. 2. (a) Cavity output spectra for pure He (dashed line) and pure  $\text{N}_2$  (red line). The calibrated mirror reflectivity is also shown (black line). (b) Extinction caused by Rayleigh scattering of pure He and  $\text{N}_2$ .

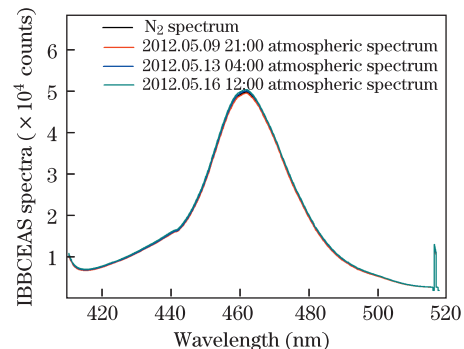


Fig. 3. Comparison of IBBCEAS spectra measured at different times and  $\text{N}_2$  spectrum. Peak intensities of these spectra fluctuate all within 1%, which shows that aerosols are almost absent in the cavity.

with IBBCEAS. The absorptions caused by aerosols and water vapor are negligible because of the PTFE filter and silica gel that prevent them from entering the cavity. The measurements of local (Hefei city) aerosols by Li *et al.*<sup>[21]</sup> show very high aerosol concentrations. Figure 3 illustrates that the difference in atmospheric spectral intensities and N<sub>2</sub> reference spectrum is very small (less than 1%), suggesting that the aerosols have been effectively filtered. Except those of the aerosols, changes in the intensity are usually negligible because of the absorptions of atmospheric trace gases, especially when the reflectivity of the mirrors is moderate. To demonstrate the performance of the filter, we compared two atmospheric spectra acquired with and without the filter. A remarkable decrease ( $\sim 10\%$ ) in the intensity occurs when the filter is removed. For the ozone of typical 30 ppbv concentration in the atmosphere, the maximum absorption is  $3.4 \times 10^{-10} \text{ cm}^{-1}$  at 462 nm<sup>[22]</sup>, where the absorption cross-section is  $4.5 \times 10^{-22} \text{ cm}^2/\text{mol}$ . The maximum absorption cross-section of O<sub>2</sub>-O<sub>2</sub> is  $6 \times 10^{-46} \text{ cm}^5/\text{mol}^2$  at 446 nm<sup>[23]</sup>, which yields peak absorption of  $1.7 \times 10^{-9} \text{ cm}^{-1}$  for O<sub>2</sub>-O<sub>2</sub> in the atmosphere. Generally, the standard deviation of the fitting residual spectrum accounts for the detection sensitivity of IBBCEAS instrument. The fitting results of NO<sub>2</sub> samples before measurements show that the detection sensitivity of our instrument is at  $10^{-8} \text{ cm}^{-1}$  level. Thus, only NO<sub>2</sub> absorption is included in the spectral range from 443 to 470 nm.

Figure 4 shows an example of atmospheric NO<sub>2</sub> concentration retrieval. The absorption spectrum of NO<sub>2</sub> was recorded with an acquisition time of 90 s. The NO<sub>2</sub> concentration was retrieved by nonlinear least-square fitting reference absorption cross-sections. These cross-sections were obtained by convoluting the cross-sections of Voigt *et al.*<sup>[24]</sup> with instrument function of spectrometer to absorption coefficient. Figure 4 illustrates that the NO<sub>2</sub> concentration and the standard deviation of residual spectrum are  $32.3 \pm 0.4 \text{ ppbv}$  and  $9.6 \times 10^{-9} \text{ cm}^{-1}$ , respectively. The corresponding uncertainty is only from the fitting algorithm, excluding the systematic errors. The measurement error of the IBBCEAS instrument mainly included the error of factor  $(1-R(\lambda))$  ( $\sim 12\%$ ) and the error of NO<sub>2</sub> cross-sections ( $\sim 5\%$ ). The total measurement error for NO<sub>2</sub> is approximately 13%.

If an optical cavity is used to detect trace gases, some losses, such as inlet or wall in the cell losses, should be sometimes considered. Other studies<sup>[25]</sup> have shown that both losses of NO<sub>2</sub> are negligible. In addition, Kebabian *et al.*<sup>[26]</sup> observed that the filter and dryer had no effect on the measured NO<sub>2</sub> concentration. Therefore, NO<sub>2</sub> concentrations, excluding these losses, are determined.

Figure 5 shows the atmospheric NO<sub>2</sub> values measured with the IBBCEAS instrument. During the seven-day measurement period, NO<sub>2</sub> concentrations range from 1 to 35 ppbv. The standard deviations of the fitting residual spectra range from  $6.8 \times 10^{-9}$  to  $1.3 \times 10^{-8} \text{ cm}^{-1}$ , and the average standard deviation is  $9.0 \times 10^{-9} \text{ cm}^{-1}$ . Assuming that the detection limit is twice the average standard deviation ( $2\sigma$ ) of these fit residuals, the detection limit for the IBBCEAS instrument is approximately 1.8 ppbv.

In field application, cavity mirrors may be contami-

nated by dust or pollutant deposition, resulting in reflectivity degradation. Mirrors usually should be protected from contaminants, for example, by purging mirrors using dry air or N<sub>2</sub> gas streams. Our mirrors are not purged because its reflectivity is moderate and is not as vulnerable to environmental pollution compared with high reflectivity mirrors. A filter is used to prevent atmospheric aerosols from entering the cell. No degradation of mirror reflectivity is observed by comparing the two spectra of pure N<sub>2</sub> acquired before and after the measurements. During the seven-day period, mirror reflectivity was calibrated once before the measurements.

To verify the results of the IBBCEAS instrument, an LP-DOAS system was used to measure simultaneously atmospheric NO<sub>2</sub>. The LP-DOAS instrument consisted of a Cassegrain telescope, which was used to send a parallel beam of light from an Xe-arc lamp (150 W, Osram, Germany) onto a retroreflector at a distance of 350 m. The light returning from the retroreflector was received by the same telescope and, through a fiber, fed into a 300-mm spectrometer (WDM1-3, Beijing Optics Instrument, China) with a PDA (Hamamatsu, Japan) detector. The LP-DOAS instrument was located at the same floor (18-m height above the ground) as the IBBCEAS instrument, and the distance between them was approximately 30 m. LP-DOAS measurements of NO<sub>2</sub> were observed in the spectral range of 330–365 nm with a spectral resolution

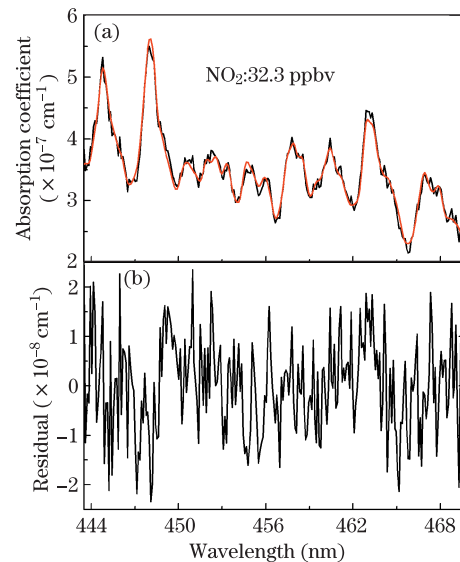


Fig. 4. (a) Measured (black line) and fitted (red line) absorption spectra of  $32.3 \pm 0.4 \text{ ppbv}$  NO<sub>2</sub> in the atmosphere with an acquisition time of 90 s. (b) Residual spectrum with a standard deviation of  $9.6 \times 10^{-9} \text{ cm}^{-1}$ .

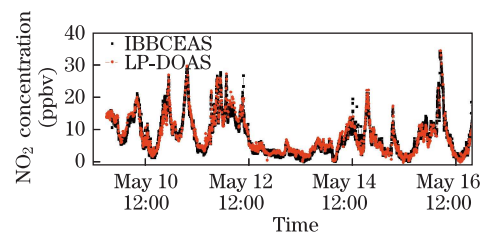


Fig. 5. Time series of simultaneous measurements of atmospheric NO<sub>2</sub> measured by the IBBCEAS instrument and a commercial LP-DOAS in 2012.

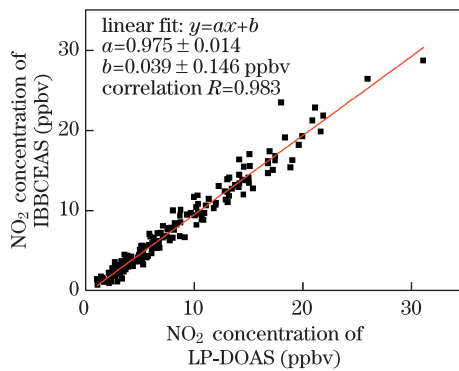


Fig. 6. Correlation of the atmospheric  $\text{NO}_2$  concentrations measured by IBBCEAS and LP-DOAS.

of 0.2 nm. Figure 5 also shows the LP-DOAS measurement results. The measurement dimensions of these instruments are different.  $\text{NO}_2$  concentrations measured by the LP-DOAS instrument are average concentrations over the folded light path, whereas those from the IBBCEAS system are point concentrations.

Figure 5 shows that the atmospheric  $\text{NO}_2$  concentrations exhibit considerable variation, which is attributable to changes in local nitrogen oxide emissions. An obvious increase in  $\text{NO}_2$  concentrations is observed every morning. Despite considerable variation in the  $\text{NO}_2$  concentrations, the IBBCEAS instrument and LP-DOAS measurements remain highly correlated. However, the IBBCEAS instrument measures more  $\text{NO}_2$  than the LP-DOAS instrument when the amount of  $\text{NO}_2$  is at the peak level. This observation is mainly attributed to intense, short-term vehicle emissions near the sampling location, which is close to a parking lot. After the peak time,  $\text{NO}_2$  is mixed well, and the difference between both measurement results becomes small. Figure 6 shows the correlation of average concentrations measured by the two instruments within 1 h. The linear regression has a slope of  $0.975 \pm 0.014$  and an intercept of  $0.039 \pm 0.146$  ppbv. Aside from the differences in measurement dimensions, discrepancies are likely attributed to differences in retrieval spectral ranges and the calibration error of mirror reflectivity of IBBCEAS. The reliability of IBBCEAS measurements of  $\text{NO}_2$  in a different spectral range has compared favorably against a range of other  $\text{NO}_2$  measurement approaches, including LIF, chemiluminescence, and CRDS<sup>[27]</sup>.

In conclusion, long-term *in situ* measurements of atmospheric  $\text{NO}_2$  using IBBCEAS with a blue LED light source are demonstrated. The IBBCEAS instrument is sensitive and accurate in measuring  $\text{NO}_2$ . If the detection sensitivity of the IBBCEAS instrument can be further improved, for example, using mirrors with higher reflectivity or longer cavity, the instrument may be used to measure other important trace gases (e.g., CHOCHO and IO) in the atmosphere.

The authors would like to acknowledge Dr. Y. Zeng for his suggestions that helped improve the language of the manuscript. This work was supported by the National Natural Science Foundation of China (Nos. 61275151 and 41275037) and the National “863” Program of China (No. 2009AA063006).

## References

1. U. Platt, D. Perner D, and H. W. Pätz, *J. Geophys. Res.* **84**, 6329 (1979).
2. U. Platt, *Phys. Chem. Chem. Phys.* **1**, 5409 (1999).
3. S. E. Fiedler, A. Hese, and A. A. Ruth, *Chem. Phys. Lett.* **371**, 284 (2003).
4. Z. Qu, C. Gao, Y. Han, X. Du, and B. Li, *Chin. Opt. Lett.* **10**, 050102 (2012).
5. S. M. Ball, J. M. Langridge, and R. L. Jones, *Chem. Phys. Lett.* **398**, 68 (2004).
6. J. M. Langridge, S. M. Ball, and R. L. Jones, *Analyst* **131**, 916 (2006).
7. T. Wu, W. Chen, E. Fertein, F. Cazier, D. Dewaele, and X. Gao, *Appl. Phys. B* **96**, 1 (2011).
8. L. Ling, P. Xie, M. Qin, R. Hu, W. Fang, N. Zheng, and F. Si, *Acta Opt. Sin.* (in Chinese) **33**, 0130002 (2013).
9. L. Ling, M. Qin, P. Xie, R. Hu, W. Fang, Y. Jiang, J. Liu, and W. Liu, *Acta Phys. Sin.* (in Chinese) **61**, 140703 (2012).
10. T. Gherman, D. S. Venables, S. Vaughan, J. Orphal, and A. A. Ruth, *Environ. Sci. Technol.* **42**, 890 (2008).
11. D. S. Venables, T. Gherman, J. Orphal, J. C. Wenger, and A. A. Ruth, *Environ. Sci. Technol.* **40**, 6758 (2006).
12. M. Triki, P. Cermak, G. Mejean, and D. Romanini, *Appl. Phys. B* **91**, 195 (2008).
13. J. Meinen, J. Thieser, U. Platt, and T. Leisner, *Atmos. Chem. Phys.* **10**, 3901 (2010).
14. R. Thalman and R. Volkamer, *Atoms. Meas. Technol.* **3**, 1797 (2010).
15. O. J. Kennedy<sup>1</sup>, B. Ouyang, J. M. Langridge, M. J. S. Daniels, S. Bauguitte, R. Freshwater, M. W. McLeod, C. Ironmonger, J. Sendall, O. Norris, R. Nightingale, S. M. Ball, and R. L. Jones, *Atmos. Meas. Technol.* **4**, 3499 (2011).
16. J. M. Langridge, S. M. Ball, A. J. L. Shillings, and R. L. Jones, *Rev. Sci. Instrum.* **79**, 123110 (2008).
17. S. Vaughan, T. Gherman, A. A. Ruth, and J. Orphal, *Phys. Chem. Chem. Phys.* **10**, 4471 (2008).
18. R. A. Washenfelder, A. O. Langford, H. Fuchs, and S. S. Brown, *Atmos. Chem. Phys.* **8**, 7779 (2008).
19. S. Shardanand and A. D. P. Rao, *NASA Technical Note* (1977).
20. M. Snee and W. Ubachs, *J. Quantum Spectrosc. Radiat. Transfer* **92**, 293 (2005).
21. J. Li, H. Wei, Q. Xu, and J. Zhan, *Opt. Prec. Eng.* (in Chinese) **20**, 1166 (2012).
22. S. Voigt, J. Orphal, K. Bogumil, and J. P. Burrows, *J. Photochem. Photobiol. A* **143**, 1 (2001).
23. G. D. Greenblatt, J. J. Orlando, J. B. Burkholder, and A. R. Ravishankara, *J. Geophys. Res.* **95**, 18577 (1990).
24. S. Voigt, J. Orphal, and J. P. Burrows, *J. Photochem. Photobiol. A* **149**, 1 (2002).
25. H. Fuchs, W. P. Dubé, S. J. Ciciora, and S. S. Brown, *Anal. Chem.* **80**, 6010 (2008).
26. P. L. Keabian, E. C. Wood, S. C. Herndon, and A. Freedman, *Environ. Sci. Technol.* **42**, 6040 (2008).
27. H. Fuchs, S. M. Ball, B. Bohn, T. Brauers, R. C. Cohen, H.-P. Dorn, W. P. Dubé, J. L. Fry, R. Häseler, U. Heitmann, R. L. Jones, J. Kleffmann, T. F. Mental, P. Müsgen, F. Rohrer, A. W. Rollins, A. A. Ruth, A. Kiendler-Scharr, E. Schlosser, A. J. L. Shillings, R. Tillmann, R. M. Varma, D. S. Venables, G. Villena Tapia, A. Wahner, R. Wegener, P. J. Woodlridge, and S. S. Brown, *Atmos. Meas. Technol.* **3**, 21 (2010).